Journal of Molecular Structure 993 (2011) 219–224

Contents lists available at ScienceDirect

Journal of Molecular Structure

journal homepage: www.elsevier.com/locate/molstruc

Varying the microstructural properties of ZnO particles using different synthesis routes

Ankica Šarić, Svetozar Musić *, Mile Ivanda

Ruđer Bošković Institute, P. O. Box 180, Bijenička cesta 54, HR-10002 Zagreb, Croatia

ARTICLE INFO

Article history:
Available online 16 October 2010

Keywords:
ZnO
FT-IR
Raman
FE-SEM

ABSTRACT

The hydrolysis at 90 °C of zinc acetylacetonate [$Zn(acac)_2$] in solutions containing sodium hydroxide and trisodium citrate was monitored using Raman and FT-IR spectroscopies and field emission scanning electron microscopy. The size and shape of the precipitated particles depended on the initial mole ratio [$Zn(acac)_2$]/[Na_3-citrate] and initial NaOH concentration. The conditions for precipitation of square plate-like particles or thin foils were determined. Nanosize ZnO particles of good uniformity were obtained by heating square plate-like particles or thin foils at 300 °C. With additional heating at 600 °C larger particles were obtained. These particles showed the Raman bands at 332, 384, 413, 438, 540 and 583 cm^{-1}, which were assigned to wurtzite-type ZnO. For the initial mole ratio [$Zn(acac)_2$]/[Na_3-citrate] = 1:0.5 and at concentration of 1×10^{-2} M NaOH the ZnO particles of different shapes were obtained which consisted of primary nanosize particles with chemically bonded citrate groups.

1. Introduction

In the last decade a rapid increase in the number of publications dealing with the synthesis of ZnO particles and thin films and their properties has been noted [1]. This is understandable in view of very important applications of ZnO materials. For example, ZnO materials have found use in both traditional technologies (paints, catalysts, rubber and cosmetics), and in advanced technologies (mechanical actuators, piezoelectric and gas sensors, photodetectors, LED's, transistors, etc.) It should be mentioned that many applications of ZnO depend on the nanostructure of ZnO particles or thin films. Generally, it is possible to change the size and shape, as well as other properties of ZnO particles by varying the synthesis procedures.

Musić et al. [2] investigated the influence of synthesis procedure on the formation and properties of ZnO. ZnO failed to crystallize through the hydrothermal treatment of the $Zn(NO_3)_2$ aqueous solution in decomposing urea at 160 °C; hydrozincite was formed instead. On the other hand, nanosize ZnO particles were instantaneously precipitated by the addition of tetramethylammonium hydroxide (TMAH) to the ethanolic solution of zinc acetate dihydrate at pH ~ 14. The precipitates obtained by an abrupt addition of the concentrated NH_4OH solution to the $Zn(NO_3)_2$ solution consisted of a complex compound of the general formula $Zn_5(OH)_8(NO_3)_2(H_2O)_{2-x}(NH_3)_x$ which on additional autoclaving transformed to ZnO [3]. The aqueous suspensions produced from the zinc acetate solution with varying amounts of the NH_4OH solution were hydrothermally aged at 160 °C and the precipitates obtained were characterized by XRD, Raman, B.E.T. and TEM [4]. ZnO particles in the micron range were precipitated by dissolution/recrystallization of the starting precipitate and the rate of this transformation increased with an increase in pH from 7 to 10. Ageing of the starting aqueous suspension for 7 months at pH 10 and room temperature yielded aggregates consisting of nanosize ZnO particles (~20 to ~60 nm). These works [2–4] were continued with the investigation [5] of the formation of ZnO particles by mixing concentrated aqueous $Zn(NO_3)_2$ and NaOH solutions. At 160 °C and pH ~ 6, plate-like $Zn_5(OH)_8(NO_3)_2(H_2O)_2$ were obtained which quickly transformed into ZnO via a dissolution/recrystallization process yielding particles of different shapes based on the hexagonal prism. $Zn_5(OH)_8(NO_3)_2(H_2O)_2$ particles precipitated at pH ~ 6 were stable up to 6 months of ageing at 20 °C. Only ZnO particles precipitated at 160 or 20 °C at pH ~ 13. All ZnO particles thus obtained were plate-like and their size depended on the time of ageing. Musić et al. [6] precipitated the $Zn_5(CO_3)_2(OH)_6$ precursor and then the precursor was converted to nanosize ZnO particles at 300 °C. The size of these ZnO particles increased to ~100 nm upon additional heating at 600 °C. The obtained ZnO particles showed a pseudospherical shape; however, their basic structure was based on the hexagonal space group. Precipitation of Zn^{2+} ions in the decomposing HMTA (hexamethylenetetramine) at 90 °C yielded ZnO particles in the micron range and these particles were strongly elongated in the direction of the crystallographic *c*-axis. Nanosize ZnO particles were prepared by rapid hydrolysis of zinc 2-ethylhexanoate dissolved in 2-propanol by adding the TMAH aqueous solution [7]. XRD showed an

* Corresponding author. Tel.: +385 1 45 61 094; fax: +385 1 46 80 098.
E-mail address: music@irb.hr (S. Musić).

0022-2860/$ - see front matter © 2010 Elsevier B.V. All rights reserved.
doi:10.1016/j.molstruc.2010.10.018

average value of 25–35 nm for the basal diameter of supposed cylinder (prism)-shaped crystallites, whereas the height of these crystallites was 35–45 nm. TEM showed that the majority of ZnO particles were 20–50 nm in size, thus indicating that the crystallite and particle sizes were approximately equal. The conditions for the formation of nanosize ZnO particles by thermal decomposition of zinc acetylacetonate monohydrate were also investigated [8].

As a follow-up to our previous investigations [2–8] we present some novel results obtained by the hydrolysis of zinc acetylacetonate in the presence of citrates. The conditions for the preparation of nanosize ZnO particles have been identified. Samples were characterized with Raman and FT-IR spectroscopies, as well as field emission scanning electron microscopy.

2. Experimental

2.1. Sample preparation

All the chemicals used in the experiments were of analytical purity. Zinc acetylacetonate monohydrate ($Zn(C_5H_7O_2)_2\cdot H_2O$) supplied by *Alfa Aeser*®; trisodium citrate ($Na_3C_6H_5O_7\cdot 5½H_2O$) supplied by *Merck*, and C_2H_5OH and NaOH supplied by *Kemika* were used. Twice distilled water was prepared in own laboratory.

The experimental conditions for sample preparation are given in Table 1. Different amounts of trisodium citrate were dissolved in 200 ml of 2×10^{-3} M NaOH solution (samples S1–S3) or 1×10^{-2} M NaOH solution (sample S4) at room temperature. Then 2.00 g Zn $(acac)_2\cdot H_2O$ was added to each of the above transparent solutions. The formed milky suspensions were vigorously shaken for ~15 min, then heated at 90 °C for 1–7 days. After a proper ageing time, the isolated precipitates were washed several times with ethanol and twice distilled water using ultracentrifuge, then dried for 48 h at 110 °C. The precipitation systems for mole ratio $[Zn(acac)_2]/[Na_3\text{-citrate}]$ = 1:0.6 to 1:1 and at concentration of 2×10^{-3} M NaOH were also prepared. However, for mole ratios 1:0.6 and 1:0.75 the precipitation was delayed for more than 1 day and for mole ratio 1:1 the precipitation was absent. Selected samples were thermally treated at 300 °C for 4 h and additionally at 600 °C for 4 h.

2.2. Instrumentation

The Raman spectra were recorded at room temperature using the double subtractive configuration of a *Horiba Jobin Yvon* T64000 triple monochromator. The 514.5 nm laser excitation line beam of the *Coherent* argon ion laser was used.

The FT-IR spectra were recorded using a *Perkin Elmer* spectrometer, model 2000. The FT-IR spectrometer was coupled to a personal computer loaded with the IRDM (IR Data Manager) program. The specimens were pressed into the pellets using spectroscopically pure KBr as a matrix.

The FE-SEM images were taken using the *JEOL* field emission scanning electron microscope JSM-7000F. Specimens were not coated with a conductive layer.

The representative results of these measurements are shown below.

Table 1
Experimental conditions for the preparation of samples.[a]

Sample	$[Zn(acac)_2]/[Na_3\text{-citrate}]$	[NaOH]/M	t_{ageing}/days	pH_{final}
S1	1:0.5	2×10^{-3}	1	6.91
S2	1:0.5	2×10^{-3}	7	5.81
S3	1:0.1	2×10^{-3}	1	6.08
S4	1:0.5	1×10^{-2}	1	7.51

[a] Each precipitation system was prepared in 200 ml volume and contained 2.00 g of zinc acetylacetonate monohydrate.

3. Results and discussion

3.1. Raman and FT-IR spectroscopies

Raman spectroscopy is a useful technique in studying ZnO particles and thin ZnO films. It is useful not only in the identification of ZnO phase but also in the investigation of some effects originating from particle size and shape, crystal disorder, doping, etc. Damen et al. [9] investigated the Raman effect on ZnO crystals in the mm size range. The authors measured two E_2 vibrations at 101 and 437 cm^{-1}; one transverse A_1 at 381 cm^{-1}, the other transverse E_1 at 407 cm^{-1}, with one longitudinal E_1 at 583 cm^{-1}. Calleja and Cardona [10] also investigated the Raman effect on a ZnO single crystal. The resonance effect of the Raman scattering by E_2, A_{1T}, E_{1L} and E_{1T} phonons and several second-order features have been investigated for ZnO with photon energies between 1.6 and 3 eV. Raman spectroscopy was used by Exarhos and Sharma [11] in the investigation of wurtzite (ZnO) films. It was concluded that these films exhibited a certain degree of residual tensile stress, as inferred from the E_2 Raman shift relative to the single crystal position of this mode.

The Raman spectra of selected samples, prepared in the present work, are shown in Figs. 1 and 2. Fig. 1 shows the Raman spectrum

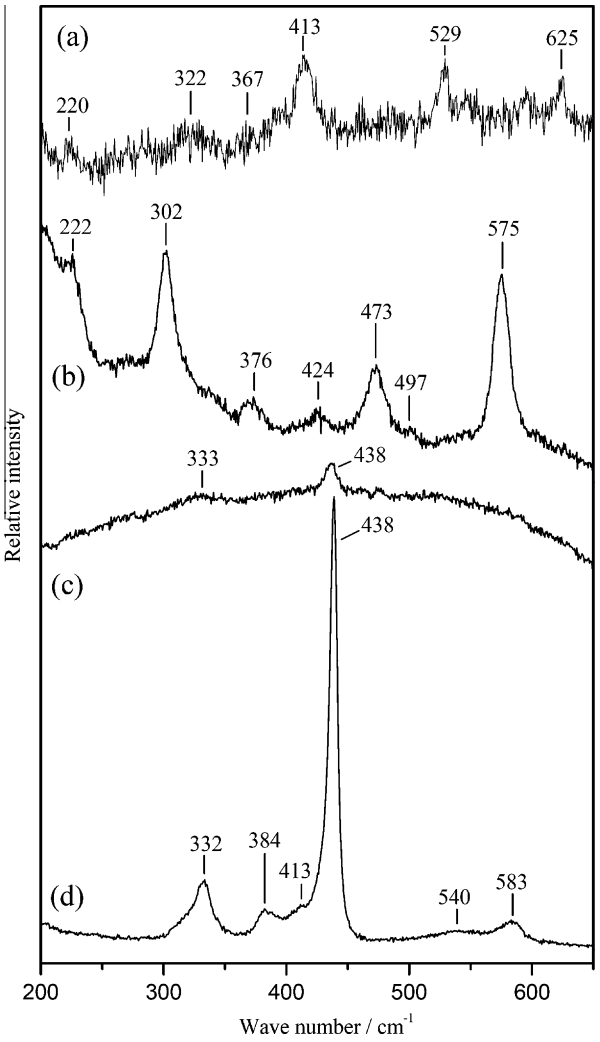

Fig. 1. Characteristic parts of the Raman spectra of (a) trisodium citrate ($Na_3C_6H_5O_7\cdot 5½H_2O$), (b) sample S2, (c) sample S2 upon heating at 300 °C, and (d) sample S2 upon heating at 600 °C.

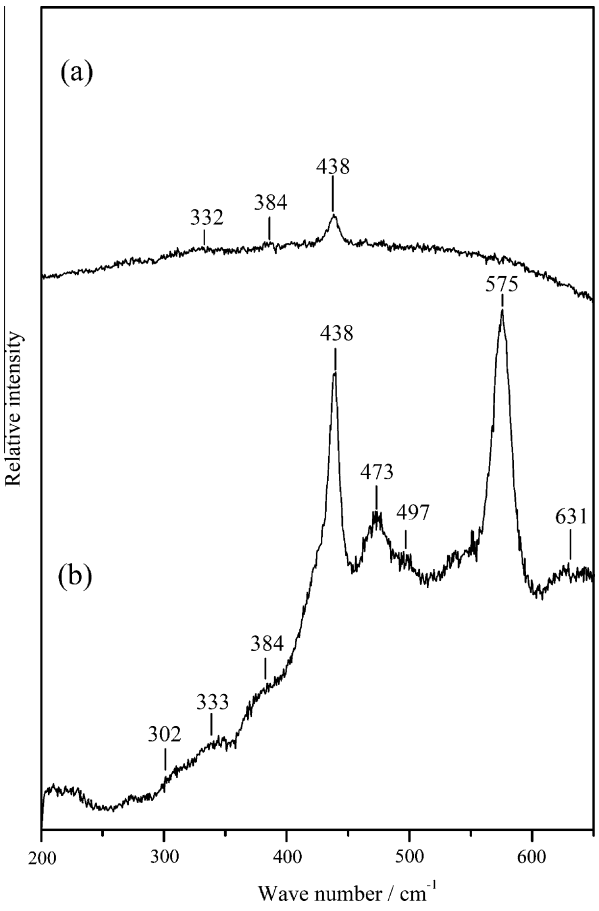

Fig. 2. Characteristic parts of the Raman spectra of (a) sample S3 upon heating at 300 °C, and (b) sample S4.

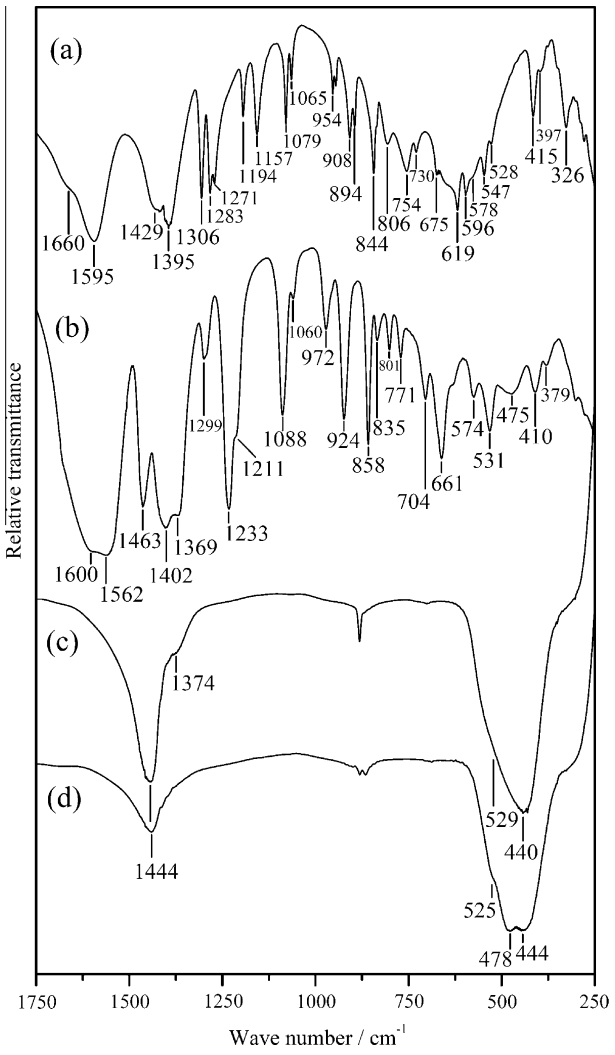

Fig. 3. Characteristic parts of the FT-IR spectra of (a) trisodium citrate ($Na_3C_6H_5O_7{\cdot}5½H_2O$), (b) sample S2, (c) sample S2 upon heating at 300 °C, and (d) sample S2 upon heating at 600 °C.

of sample S2 precipitated for the mole ratio [$Zn(acac)_2$]/[Na_3-citrate] = 1:0.5 and 7 days of heating at 90 °C. The Raman spectrum of the starting salt trisodium citrate is also shown for comparison. The main feature of the Raman spectrum of sample S2 are dominant Raman bands at 302, 473 and 575 cm^{-1} which are not present in the reference spectrum of trisodium citrate. Acetylacetonate groups can be eliminated because they are washed out from the precipitate. Taking into account the final pH 5.81 and a high affinity of citrates to ZnO/$Zn(OH)_2$ surfaces, it is realistic to suppose that these dominant Raman bands belong to the newly formed ZnO/$Zn(OH)_2$–citrate complex in the solid state. However, at high pH values there is a strong competition between zincate and citrate ions resulting in ZnO crystallization. Vibrational spectra of citrate groups were discussed elsewhere [12–15]. Upon heating of the isolated precipitate S2 at 300 °C no citrate groups are visible, while two broad Raman bands at 438 and 333 cm^{-1} are visible, which can be assigned to very small ZnO particles of probably a lower degree of crystallinity. The Raman spectrum of sample S2 after its heating at 600 °C showed bands typical of ZnO (hexagonal symmetry of wurtzite).

Fig. 2 shows the Raman spectra of (a) sample S3 precipitated for mole ratio [$Zn(acac)_2$]/[Na_3-citrate] = 1:0.1 and additionally heated at 300 °C, and (b) sample S4 precipitated for mole ratio [$Zn(acac)_2$]/[Na_3-citrate] = 1:0.5 and the final pH 7.51. The spectrum of sample S3 heated at 300 °C is characterized by broad bands centered at 438, 384 and 332 cm^{-1}. This spectrum can be assigned to nanostructured ZnO of probably a lower degree of crystallinity. The Raman spectrum of sample S4 showed the main features corresponding to ZnO phase; however, the spectral lines were broadened, which can be a sign of very small particles or low crystallinity. The additional Raman bands indicate chemically bonded citrate groups to the precipitate.

Infrared spectroscopy was earlier used to characterize ZnO. For example, Boccuzzi et al. [16] used IR spectroscopy to investigate the surface behaviour of a well-crystallized ZnO, particularly sensitive to surface reactions. The impact of temperature and atmosphere, during the heating of ZnO on the corresponding IR spectrum was also investigated [17]. Hayashi et al. [18] compared the recorded and calculated spectra of ZnO and found that ZnO showed three distinct absorption bands located between bulk TO-phonon frequency ($\omega_{T\|}$) and LO-phonon frequency ($\omega_{L\perp}$). In addition to that, these bands shifted towards lower frequencies when the permittivity of the surrounding medium was increased. Andrés-Vergés et al. [19] discussed the dependence of the IR spectrum of ZnO particles on various geometrical shapes and suggested the origin of an IR band at 494 cm^{-1}.

Figs. 3 and 4 show characteristic parts of the FT-IR spectra of selected samples. The FT-IR spectrum of sample S2 is in accordance with the conclusion based on the corresponding Raman spectrum concerning the formation of ZnO/$Zn(OH)_2$–citrate complex in the solid state. A broad peak at 475 cm^{-1} can be assigned to the ZnO phase. The citrate groups are not only confined to the surface of

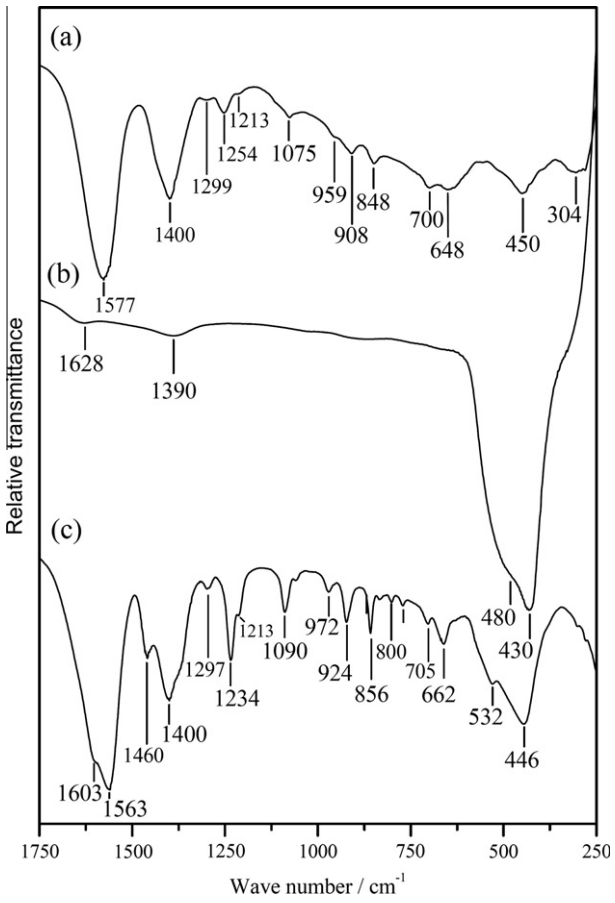

Fig. 4. Characteristic parts of the FT-IR spectra of (a) sample S3, (b) sample S3 upon heating at 300 °C, and (c) sample S4.

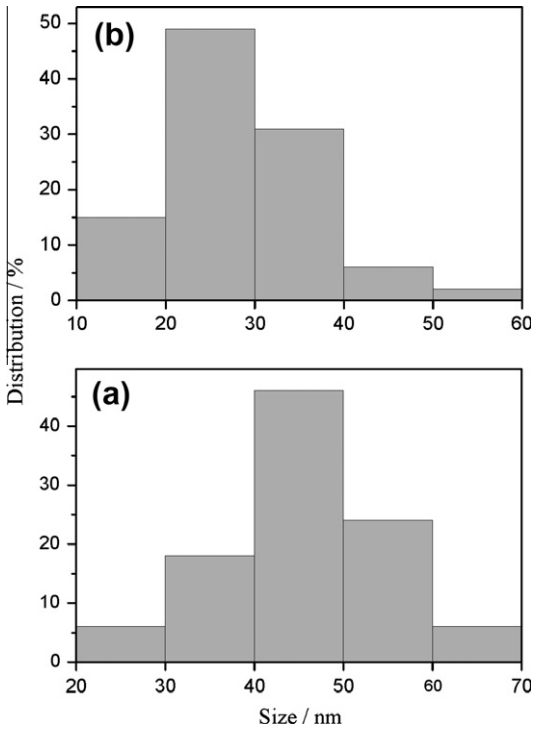

Fig. 6. Particle size distributions of (a) sample S2 heated at 300 °C, and (b) sample S3 heated at 300 °C.

ZnO particles, but they can be bonded to ZnO in the bulk of these particles. Heating of sample S2 at 300 °C yielded an intensive and broad IR band at 440 cm^{-1} with a shoulder at 529 cm^{-1}. In this spectrum the IR bands at 1444 and 1374 cm^{-1} are also visible, indicating that COO groups are not completely removed. The relative intensity of the band at 1444 cm^{-1} for ZnO sample S2 heated at 600 °C is significantly decreased.

Fig. 4 shows the residue of citrate bonded to ZnO particles (sample S3) which are characterized by a broad band at 450 cm^{-1}. Upon heating of sample S3 at 300 °C the corresponding FT-IR spectrum

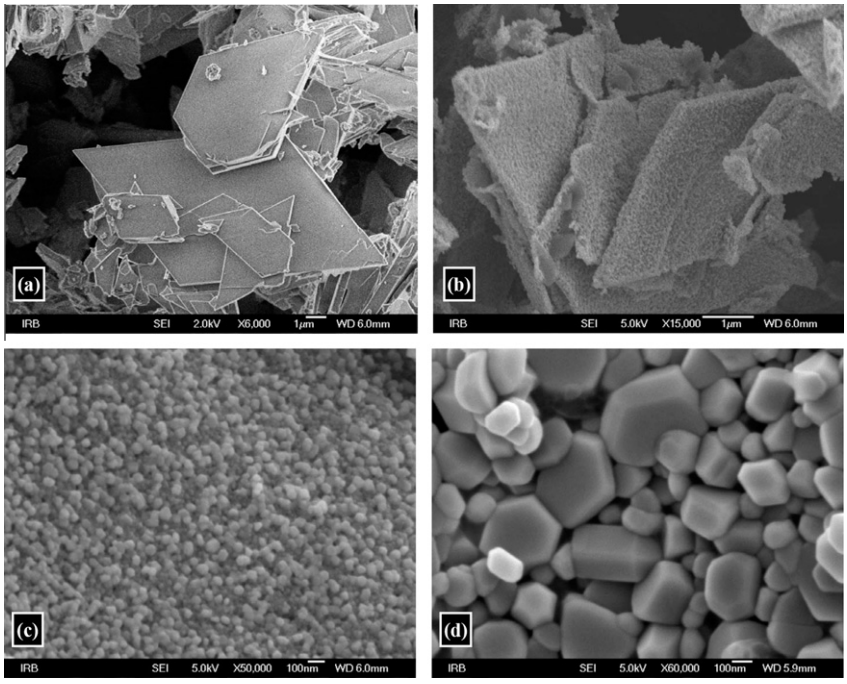

Fig. 5. FE-SEM images of (a) sample S2, (b, c) sample S2 upon its heating at 300 °C (two details), and (d) sample S2 upon heating at 600 °C.

showed an IR band at 430 cm^{-1} with a shoulder at 480 cm^{-1}. The same FT-IR spectrum showed an IR band at 1390 cm^{-1} due to the residual CO bond and an IR band at 1628 cm^{-1} due to the bending vibration of H_2O moisture. ZnO particles of sample S4 showed an IR band at 446 cm^{-1} and a shoulder at 532 cm^{-1} plus additional bands which can be assigned to the presence of citrate groups.

3.2. FE-SEM

In reference literature there are different reports about the influence of citrates on the formation of ZnO particles (crystals) and their shape. Cho et al. [20] investigated the effect of citrates on ZnO precipitation from zinc acetate solutions. Citrates were added in the chemical form as triethyl citrate, tripotassium citrate, trisodium citrate and triammonium citrate. Triethyl citrate was a less effective suppressor of the ZnO crystal growth than tripotassium and trisodium citrate. Triammonium citrate was also an effective suppressor of the ZnO [0 0 0 1] crystal growth. Zhang et al. [21] observed the citrate-induced hierarchical growth of secondary hexagonal plates with thickness from ~250 to ~320 nm. Wu et al. [22] precipitated ZnO nanoparticles at pH 11 and the formation of these particles was studied through the competition between $[Zn(C_6H_5O_7)_4]^{10-}$ citrate complexes and $[Zn(OH)_4]^{2-}$ hydroxy complexes. The effects of citrates on the morphology of nanostructured ZnO powders and films were also investigated by Garcia and Semancik [23] and Choppali and Gorman [24], respectively.

All samples prepared in the present work were inspected with FE-SEM and the images of selected samples will be shown here. The main feature of samples S1 and S2 are particles in the form of square plates. Fig. 5a shows square plate-like particles of sample S2. Generally, ZnO is easily forming hexagonal plate-like particles when [0 0 0 1] planes are blocked with specifically adsorbed ions or molecules. However, in the present case square plate-like particles are obtained. Recently, Cho et al. [25] reported a synthesis of thin ZnO plates without the assistance of specific molecules. The authors suggested that the square plane obtained for square plate-like particles belongs to the crystallographic $[2\bar{1}\bar{1}0]$ direction. Obviously, the preferential adsorption of citrates under pH values near neutral in the present experiments created conditions for the formation of square plate-like particles or thin ZnO foils (plates). Square WO_3 nanoplates were precipitated by the hydrothermal method using citric acid as an assistant agent [26]. Upon heating of sample S2 at 300 °C the starting morphology was preserved (Fig. 5b); however, it was quite clear that the particles produced at 300 °C consisted of nanosize ZnO particles, as documented with Fig. 5c at higher magnification. Fig. 6a shows particle size distribution of ZnO particles with maximum size at 40 to 50 nm. Upon additional heating of sample S2 at 600 °C the nanosize ZnO particles significantly grew and the hexagonal symmetry of these particles was well visible (Fig. 5d). Fig. 7 shows the FE-SEM images of sample S3 and after its heating at 300 °C. The particles of sample S3 are different in relation to samples S1 and S2, i.e., thin foils are obtained instead of square plate-like particles. Upon

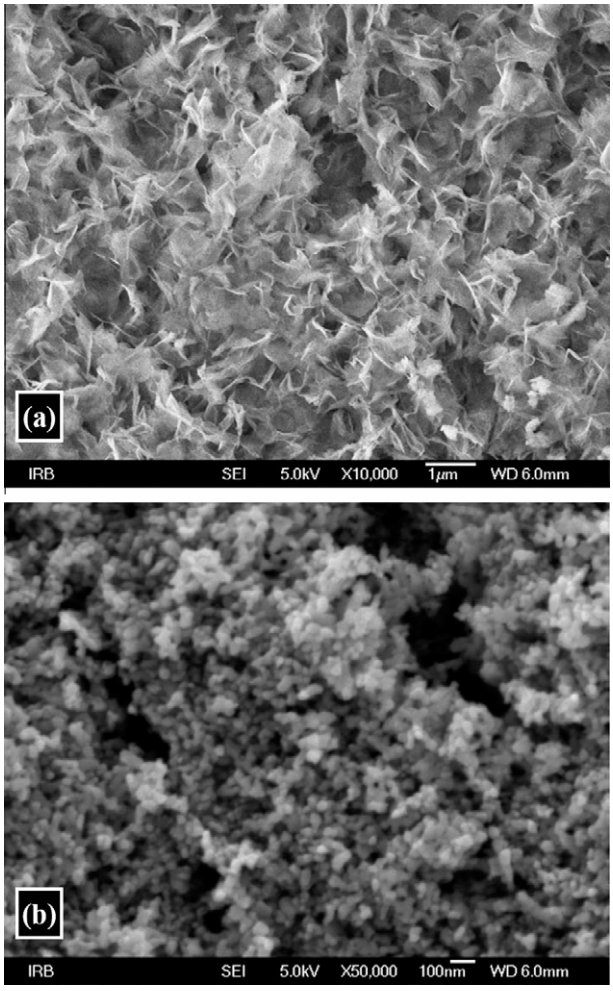

Fig. 7. FE-SEM images of (a) sample S3, and (b) sample S3 upon its heating at 300 °C.

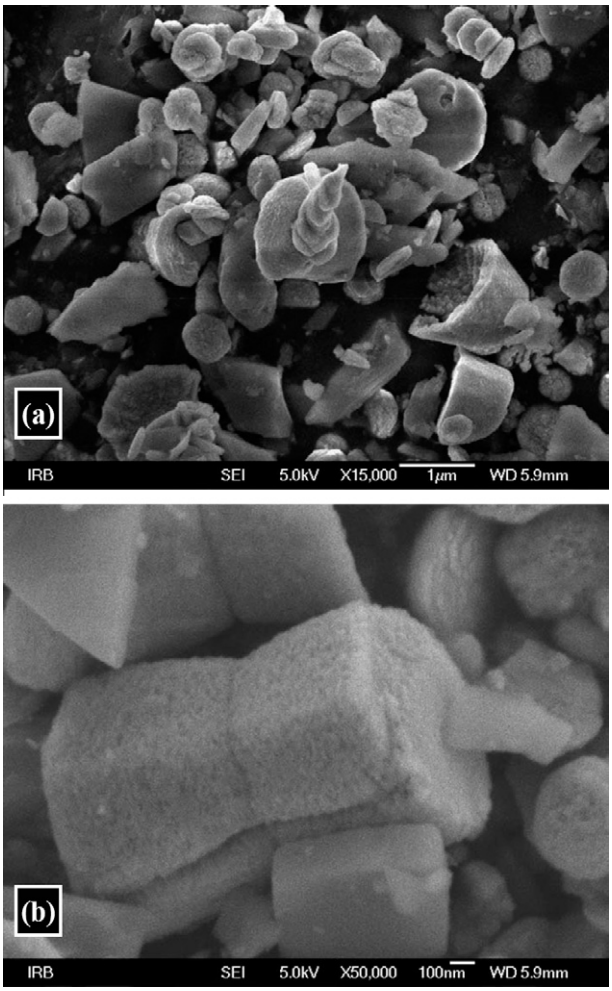

Fig. 8. FE-SEM images of sample S4 with two details (a, b).

heating of sample S3 at 300 °C, nanosize ZnO particles were produced with maximum particle size distribution at 20–30 nm (Fig. 6b). For the mole ratio $[Zn(acac)_2]/[Na_3\text{-citrate}] = 1{:}0.5$ and 1×10^{-2} M NaOH solution particles of very different shapes (Fig. 8) were obtained compared with samples S1 and S2. These particles were aggregates of nanosize ZnO particles. Obviously, an increase in the initial NaOH concentration (1×10^{-2} M NaOH) had also strong influence on the shape of the particles.

4. Conclusion

The hydrolysis of zinc acetylacetonate $[Zn(acac)_2]$ in the solutions containing sodium hydroxide and trisodium citrate was monitored for 1–7 days at 90 °C. For the initial mole ratio $[Zn(acac)_2]/[Na_3\text{-citrate}] = 1{:}0.5$ and at concentration of 2×10^{-3} M NaOH square plate-like particles were obtained between 1 and 7 days of ageing. Raman and FT-IR spectroscopies indicated a strong presence of citrate groups chemically bonded to external and internal surfaces of these square plate-like particles. Three strong Raman bands at 302, 473 and 575 cm^{-1} were found and they were assigned to $ZnO/Zn(OH)_2$–citrate complex in the solid state. For the initial mole ratio $[Zn(acac)_2]/[Na_3\text{-citrate}] = 1{:}0.1$ and 2×10^{-3} M NaOH thin ZnO foils precipitated and FT-IR spectroscopy showed chemisorption of citrate groups on these particles. By heating square plate-like particles or thin ZnO foils at 300 °C, nanosize ZnO particles of good uniformity were produced. With additional heating at 600 °C larger particles (~100 nm and higher) of hexagonal symmetry were produced and they were characterized by Raman bands at 332, 384, 413, 438, 540 and 583 cm^{-1}, which can be assigned to wurtzite-type ZnO. For the initial molar ratio $[Zn(acac)_2]/[Na_3\text{-citrate}] = 1{:}0.5$ and at concentration of 1×10^{-2} M NaOH ZnO particles of very different shapes were produced. These particles were aggregates of primary nanosize ZnO particles which also contained chemically bonded citrate groups.

References

[1] S. Baruah, J. Dutta, Sci. Technol. Adv. Mater., 10 (2009) doi:10.1088/1468-6996/10/1/013001.
[2] S. Musić, S. Popović, M. Maljković, Đ. Dragčević, J. Alloys Compd. 347 (2002) 324.
[3] S. Musić, Đ. Dragčević, M. Maljković, S. Popović, Mater. Chem. Phys. 77 (2002) 521.
[4] S. Musić, Đ. Dragčević, S. Popović, M. Ivanda, Mater. Lett. 59 (2005) 2388.
[5] S. Musić, Đ. Dragčević, S. Popović, J. Alloys Comp. 429 (2007) 242.
[6] S. Musić, A. Šarić, S. Popović, J. Alloys Comp. 448 (2008) 277.
[7] M. Ristić, S. Musić, M. Ivanda, S. Popović, J. Alloys Comp. 397 (2005) L1.
[8] S. Musić, A. Šarić, S. Popović, Ceram. Int. 36 (2010) 1117.
[9] T.C. Damen, S.P.S. Porto, B. Tell, Phys. Rev. 142 (1966) 570.
[10] J.M. Calleja, M. Cardona, Phys. Rev. B 16 (1977) 3753.
[11] G.J. Exarhos, S.K. Sharma, Thin Solid Films 270 (1995) 27.
[12] P. Tarakeshwar, S. Manogaran, Spectrochim. Acta 50A (1994) 2327.
[13] R.I. Bickley, H.G.M. Edwards, R. Gustar, S.J. Rose, J. Mol. Struct. 246 (1991) 217.
[14] G.E. Tobón-Zapata, O.E. Piro, S.B. Etcheverry, E.J. Baran, Z. Anorg. Allg. Chem. 624 (1998) 721.
[15] G. Vanhoyland, J. Pagnaer, J. D'Haen, S. Mullens, J. Mullens, J. Solid State Chem. 178 (2005) 166.
[16] F. Boccuzzi, E. Borello, A. Chiorino, A. Zecchina, Chem. Phys. Lett. 61 (1979) 617.
[17] F. Boccuzzi, C. Morterra, R. Scala, A. Zecchina, J. Chem. Soc. Faraday Trans. 2: Mol. Chem. Phys. 77 (1981) 2059.
[18] S. Hayashi, N. Nakamori, H. Kanamori, Y. Yodogawa, K. Yamamoto, Surf. Sci. 86 (1979) 665.
[19] M. Andrés-Vergés, A. Mifsud, C.J. Serna, J. Chem. Soc. Faraday Trans. 86 (1990) 959.
[20] S. Cho, J.-W. Jang, S.-H. Jung, B.R. Lee, E. Oh, K.-H. Lee, Langmuir 25 (2009) 3825.
[21] T. Zhang, W. Dong, M. Keeter-Brewer, S. Konar, R.N. Njabon, Z.R. Tian, J. Am. Chem. Soc. 128 (2006) 10960.
[22] C. Wu, X. Qiao, J. Chen, H. Wang, Mater. Chem. Phys. 102 (2007) 7.
[23] S.P. Garcia, S. Semancik, Chem. Mater. 19 (2007) 4016.
[24] U. Choppali, B.P. Gorman, J. Lumin. 128 (2008) 1641.
[25] S. Cho, J.-W. Jang, J.S. Lee, K.-H. Lee, Langmuir 26 (2010) 14255.
[26] X. Su, F. Xiao, Y. Li, J. Jian, Q. Sun, J. Wang, Mater. Lett. 64 (2010) 1232.